# Global plasma model of a Microwave Electrothermal Thruster for self-consistent performance calculations

M. Lauriola[1], M. Nava[2], A. Maffini[1], F. Maggi[2], M. Passoni[1]

[1] *Politecnico di Milano, Dipartiment di Energia, Milan, Italy*

[2] *Politecnico di Milano, Dipartimento di Scienze e Tecnologie Aerospaziali, Milan, Italy*

Although numerical multidimensional kinetic and fluid plasma models are an essential tool for device design and optimization, they often require significant computational resources and times, making challenging to predict plasma properties across a wide range of parameters. In contrast, global models (despite relying on simplifying assumptions) enable the study of plasma with complex chemistry across a broad range of operating conditions, within reasonable computational time. As a result, they are widely used in various areas of plasma physics. This study aims to advance current state-of-the-art models by including the effect of gas and cavity wall temperatures heating, usually neglected. The developed model is applied to analyze the plasma discharge of an electric thruster known as Microwave Electrothermal Thruster, varying chamber dimensions and specific energy. Results demonstrate the model capability to predict plasma properties and device performance, as well as their scaling with operating conditions, with computational times below 10 s.

## 1. Introduction

**Global (0D) models** are a type of fluid model that solve a set of particles (*PaBE*) and power (*PoBE*) balance equations computing time-dependent, volume-averaged plasma species densities and temperatures (excluding the momentum balance equation) [1,2]. They are fast, simple, and versatile numerical tools which offers a practical alternative to the high computational cost of multidimensional fluid or kinetic models. In fact, 0D models provide useful insights into plasmas with complex chemistry (involving many species and reactions) and help evaluate the influence of design parameters (e.g., chamber dimensions) and operating conditions (e.g., input power, mass flow rate) on plasma behavior [1]. As such, they provide guidance for the development of more complex models.

Many 0D models have been developed to study plasma chemistry, magnetically confined plasmas, or to predict electric thrusters performance [2]. However, most state-of-the-art models do not account for heavy species (ions and neutrals) heating and treat their temperature as an input. Although a few authors attempted to address this effect, which can be relevant in microwave discharges, they ignored heat transfer to the external environment or assumed a constant wall temperature, limiting the accurate assessment of the device performance [3].

This work tries to extend current state-of-the-art 0D plasma models by including a set of PaBE for each plasma species, and three PoBE accounting for electrons, heavy species, and wall temperature heating. It is applied to an electrothermal thruster known as **Microwave Electrothermal Thruster** (**MET**) using argon and helium, commonly employed in experiments. Simulations investigate the effects of mass flow rate and chamber dimensions on steady state densities and temperatures, as well as wall temperature, and are used to assess MET performance: *thrust, specific impulse, and thruster efficiency*.

## 2. The Microwave Electrothermal Thruster

The MET [4] is an electrodeless propulsive device which employs microwaves (MWs) to create and sustain a free-floating plasma. The plasma absorbs MW energy and transfers it to the swirling propellant, increasing its thermal energy. The heated propellant expands through a solid nozzle, producing thrust. The thruster cylindrical resonant cavity is divided by a *dielectric plate* into: 1) an *antenna section*, housing the MW feed, and 2) *a plasma section,* enclosed by an endplate housing the nozzle.

The cavity is excited in the $TM_{011}$ mode, providing high power density on axis and near the nozzle. Once the resonance frequency is set to match the MW generator operating frequency, the relation $f_{res} = c/(2\pi)\, \chi_{01}/R_c \sqrt{1 + (\pi/\chi_{01})^2\, \xi^2}$ can be used to compute cavity dimension. In the above equation, $c$ is the speed of light in vacuum, $\chi_{01}$ the $J_0$ Bessel's function first zero, $R_C$ the cavity radius, and $\xi = R_c/L_c$ is the *radius-to-length ratio*. When designing the cavity, two constraints must be accounted for: 1) the radius must exceed the *cut-off radius,* below which the $TM_{011}$ mode cannot be excited (computed by letting $\xi \to 0$), and 2) the ratio $\xi < 1$ to prevent off-axis unstable plasma caused by excessive power density concentrated in an annular region about the cavity axis (for $\xi = 1$, $R_c = 77\ cm$ at 2.45 GHz).

METs operating at frequencies of 0.915, 2.45, 7.5, 30 GHz and with many propellants ($He$, $Ar$, $H_2O$, $N_2$, $N_2O$, $N_2H_4$) have been designed and tested. These systems have demonstrated high versatility and throttling capability, achieving performance comparable to arcjets.

## 3. **The global plasma model**

The key equations are summarized hereafter. Further details can be found in the literature[1-3].

Each PaBE accounts for production and loss terms resulting from atomic and chemical reactions, expressed through appropriate reaction rates. Species diffusion is included through effective loss frequencies. In the MET case, neutral species being exhausted through the nozzle are removed from the chamber at a rate based on the chocked mass flow [3], computed using quasi-1D isentropic theory $K_{exh} = \dot{m}_{choked}/(n_j V)$, where $n_j$ and $T_j$ are the species j number density and temperature, V the chamber volume.

The electron PoBE balances the power absorbed by plasma electrons to losses from inelastic processes (e.g., ionization), diffusion, and elastic collisions with heavy species. This latter term serves as a source in the heavy species PoBE. This equation also includes contributions from enthalpy change ($\dot{m}\Delta h$, where $\Delta h$ is the enthalpy change) [3] and heat transfer to the external environment. Heat losses are estimated by integrating Fourier's law of conduction in a cylindrical geometry, assuming a constant volumetric power, and averaging the temperature profile (also accounting for a parabolic velocity distribution [5]. Finally, a modified lumped capacitance method is used to model wall heating [5], assuming radiative heat transfer into vacuum at 0 K.

## 4. Simulation setup

In all the simulations, the cavity operates at an input power of 1 kW. The inlet propellant is kept at 300 K, the nozzle throat radius is fixed at 0.7 mm, and wall thickness is set to 10% of cavity radius. The specific energy is varied in the range $1 - 100\ MJ/kg$. Chamber walls are assumed to be in stainless steel, with constant thermal properties. Two different design are compared: 1) 2.45 GHz ($R_c = 5$ cm, $L_c = 17.5$ cm) and 2) 7.50 GHz ($R_c = 1.6$ cm, $L_c = 5.15$ cm). For both argon and helium, the model includes only three species (X, X+, e) and five reactions: ionization, excitation, wall recombination, elastic collisions, nozzle exhaust. Simulations were run on a personal laptop and simulations time remained below 1 minute.

## 5. Results and discussion

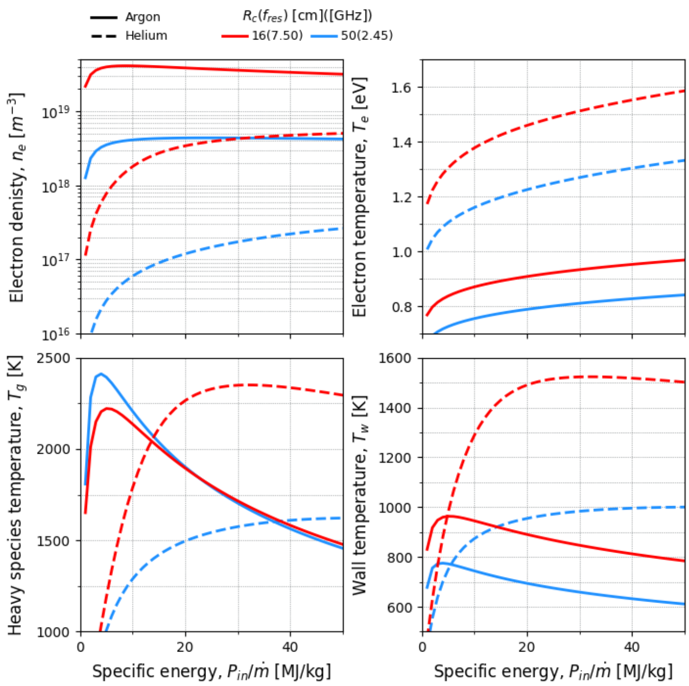


*Figure 1: Plasma properties in Argon and Helium for resonant frequencies.*

Figure 1 shows the computed plasma properties at two resonant frequencies: from the upper left to the lower right the electron density, electron temperature, heavy species temperature, wall temperature.

It can be observed that when chamber frequency increases (corresponding to a decrease in volume) both electron density and temperature increase in both gases. The increase in electron density can be attributed to the higher absorbed power density, consistent with the theory ($n_e \propto P_{abs}/V$ [1]). The rise in electron temperature is likely due to enhanced species losses at the chamber wall because of the increased surface-to-volume ratio [1].

Wall temperatures are higher in the smaller chamber ($f_{res} = 7.50$ GHz) due to higher wall heat fluxes, causing a substantial wall heating. The heat flux as a function of specific energy is displayed in Figure 2. It should be noted that, at 7.50 GHz, wall temperature exceeds the melting point of stainless steel. Hence, these results should be interpreted as purely indicative.

Gas temperatures exhibit different behavior in argon and helium plasmas. In argon, the temperature (including its peak value) decreases with increasing resonant frequency only at low specific energies, whereas in helium the temperatures are the largest in the smallest chamber at all specific energies. This difference is likely due to variation in the absorbed power density profiles between the two plasmas. As showed in the first graph of Figure 2, the

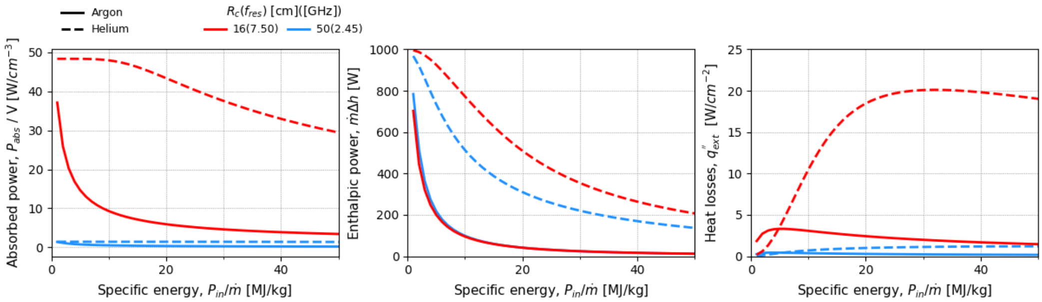


*Figure 2: Reflected MW power, enthalpic power, and heat losses in Argon and Helium, for different resonant frequencies at 1 kW.*

absorbed power density in argon drops sharply at 7.50 GHz, whereas helium exhibits a smoother dependence on specific senergy. This behavior can be justified by the larger argon plasma density and lower pressure (not shown) which can lead to significant electromagnetic power reflections. Finally, Figure 2 also displays the power spent to increase the propellant enthalpy which is larger in helium, whereas in argon is independent on chamber geometry.

## 6. **Conlcusion**

This study presents an improved 0D plasma model accounting for heavy species and wall temperature heating, testing on a thruster known as Microwave Electrothermal Thruster using propellant such as argon and helium for different cavity dimensions, across 1-100 MJ/kg specific energy range. Simulations predict plasma parameters, as well as input power partitioning into five plasma processes, within a runtime below 1 min. Results provide insights into the influence of different modelling choice and operating condition on the discharge. Future modelling activity should focus on molecular gases and different wall materials.

**Acknowledgements**

The authors thank D-Orbit s.p.a. for supporting this work.

**References**

[1] A. Hurlbatt, A. R. Gibson et al. 2017 Plasma Process. Polym. **14** 1600138
[2] L. L. Alves, A. Bogaerts et al. 2018 Plasma Sources Sci. Technol. **27** 023002
[3] F. J. Bosi 2019 Phys. Plasmas **26** 033510
[4] M. M. Micci, S. G. Bilen 2009 EUCASS Proceedings Series – Advances in Aerospace Sciences Vol . 1
[5] T. L. Bergman, A. S. Lavine et al. Fundamental of Heat and Mass Transfer 8th Ed. (John Wiley and Sons)